

# HUMAN BODY COMPOSITION: Advances in Models and Methods

*Steven B. Heymsfield and ZiMian Wang*

Obesity Research Center, Department of Medicine, St. Luke's-Roosevelt Hospital Center, Columbia University College of Physicians and Surgeons, New York, New York 10025; e-mail: SBH2@Columbia.edu

*Richard N. Baumgartner*

Clinical Nutrition Research Center, Surge Building, Room 215, University of New Mexico School of Medicine, Albuquerque, New Mexico 87133

*Robert Ross*

School of Physical and Health Education, Queen's University, Kingston, Ontario, Canada K7L 3N6

**KEY WORDS:** bioimpedance analysis, computerized axial tomography, dual-energy X-ray absorptiometry, magnetic resonance imaging, neutron activation analysis

---

## ABSTRACT

The field of human body composition research is reaching a mature stage in its development: The three interconnected areas that define body composition research—models and their rules, methodology, and biological effects—are well-defined and are actively investigated by scientists in diverse disciplines from many different nations; and methods are available for measuring all major atomic, molecular, cellular, and tissue-system level body composition components in research, clinical, and epidemiological settings. This review summarizes main body composition research concepts, examines new component-measurement methodologies, and identifies potential areas of future research.

---

## CONTENTS

INTRODUCTION .....	528
SCOPE OF BODY COMPOSITION RESEARCH .....	528
ATOMIC LEVEL .....	530
<i>Components and Their Relationships</i> .....	530

<i>Measurement Methods</i> .....	532
MOLECULAR LEVEL .....	538
<i>Components and Their Relationships</i> .....	538
<i>Measurement Methods</i> .....	540
CELLULAR LEVEL .....	548
<i>Components and Their Relationships</i> .....	548
<i>Measurement Methods</i> .....	549
TISSUE-SYSTEM LEVEL .....	549
<i>Components and Their Relationships</i> .....	549
<i>Measurement Methods</i> .....	550
METHOD SELECTION .....	554
<i>Reference Method</i> .....	554
<i>Study Method</i> .....	555
CONCLUSION .....	555

## INTRODUCTION

A daily growth hormone injection increases fat-free body mass in patients with acquired immune deficiency syndrome (AIDS) (46). What does this mean? Does the increase in fat-free body mass reflect the well-known anabolic effects of growth hormone, or does it represent the equally well-characterized fluid-retaining properties of the hormone and closely related insulin-like growth factor-1 (58)?

In elderly subjects, regular exercise increases strength and, to a small but statistically significant extent, cross-sectional thigh muscle area (21). Does the increase in skeletal muscle area, measured by magnetic resonance imaging (MRI), indicate exercise-mediated net muscle protein synthesis, or is the enlarged muscle area secondary to augmented glycogen and water retention?

These and other questions are at the center of a rapidly expanding field referred to as body composition research. This review describes important recent advances in this field, with an emphasis on examining the questions and issues posed by modern nutritional, exercise, and pharmacological therapies.

## SCOPE OF BODY COMPOSITION RESEARCH

Although more than a century old, the field of body composition research has emerged only recently as a distinct area of scientific inquiry. The main body of knowledge in this expanding area of human biology can be found in the over 3900 research articles, 18 books, and 4 international symposia proceedings related to body composition published since the early 1960s (77).

This vast and growing body of information can be organized into three distinct, interconnected areas: body composition rules; methodology; and biological effects (77). That each area interacts with the others (for example, the biological action of growth hormone on expanding extracellular fluid has


N, Ca, P, K, Na, Cl	Lipid		Adipose Tissue
H	Water		Skeletal Muscle
C		Extracellular Fluid	Visceral Organs & Residual
O	Proteins	Extracellular Solids	Skeleton
	Glycogen		
	Minerals		
<i>Atomic</i>	<i>Molecular</i>	<i>Cellular</i>	<i>Tissue-System</i>

Figure 1 Some of the main components at the first four body composition levels. (From Reference 39 with permission.)

important effects on the validity of methods used to estimate total body fat) is a central concept that should be considered when interpreting body composition research.

The body composition rule area organizes the more than 30 main body components into five distinct levels of increasing complexity: atomic, molecular, cellular, tissue system, and whole body (77). Some of the main components at the first four body composition levels are shown in Figure 1. Within this research area, investigators establish the various characteristics of body components and their quantitative relationships to one another, the “rules.” Several commonly applied rules are that 16% of protein is nitrogen (14), 77% of fat is carbon (45), and approximately two thirds of excess body weight in adults is fat (22).

An important concept when considering the five-level model is that components at successively higher body composition levels are composed of lower-level components. A classic example is that adipose tissue, a tissue-system level component, includes components such as adipocytes at the cellular level, lipids at the molecular level, and carbon at the atomic level (Figure 1). Loss or gain of adipose tissue with a new intervention reflects changes in corresponding components at the cellular, molecular, and atomic levels.

Another important concept is the existence of a body-composition steady state. During stable periods, such as with maintenance of body weight and fluid homeostasis, there are relations between components that are constant or relatively constant within an individual and between different individuals. For

**Table 1** Body composition levels and some relevant measurement methods

Level	Recently developed or improved methods	Other methods
Atomic	Neutron activation analysis	Whole-body <sup>40</sup> K counting Tracer dilution
Molecular	Bioimpedance analysis Dual energy X-ray absorptiometry Multicompartment models	Underwater weighing Infrared interactance Tracer and gas dilution
Cellular		Tracer dilution
Tissue system	Computerized axial tomography Magnetic resonance imaging	Ultrasound 24-h urinary creatinine and 3-methyl histidine excretion
Whole body		Anthropometry

example, even though fat and adipose tissue are molecular and tissue-system level components, respectively, there exists a reasonably stable relationship between the two, both within and between subjects (i.e. fat mass =  $\sim 0.80 \times$  adipose tissue mass) (72). This fundamental concept is central to development of body composition methods. That is, provided with a measured property or component, the investigator can estimate an unknown component based on assumed stable property-component or component-component relations.

In the following sections, we provide a description of each body composition level, followed by an overview of measurement methods and component relationships. Our methodology focus is on improved or recently developed technologies (Table 1).

## ATOMIC LEVEL

Elements are the fundamental building blocks of all biological organisms. About 50 of the 106 elements found in nature are also found in the human body, and many of these are required by humans for growth and health maintenance (77). Today, all 50 of these elements can be measured *in vivo* along with additional nonessential and toxic elements such as Hg, Al, Cd, and Pb.

### *Components and Their Relationships*

Four elements—O, C, H, and N—account for over 95% of body mass and with an additional seven—Na, K, P, Cl, Ca, Mg, and S—comprise over 99.5% of body mass (72, 77).

Elements maintain stable or relatively stable associations with other elements and with components at higher levels (Table 2). Several of these associations are (kg/kg): S/N = 0.062; N/protein = 0.16; C/triacylglycerol =

**Table 2** Examples of body composition models<sup>a</sup>

Level/level	Model
Atomic/atomic	TBS = 0.062 × TBN
Atomic/atomic	TBP = 0.456 × TBCa + 0.555 × TBK
Atomic/molecular	TBCa = 0.364 × Mo
Atomic/molecular	TBN = 0.16 × protein
Atomic/molecular	TBK = 0.00266 × fat-free body mass
Atomic/molecular	Carbon = 0.774 × fat
Atomic/molecular	TBS = 0.010 × protein
Atomic/cellular	TBK = 0.00469 × body cell mass
Atomic/whole body	TBH = 0.10 × BW
Molecular/molecular	TBW = 0.732 × fat-free body mass
Molecular/molecular	Glycogen = 0.044 × protein
Whole body/atomic	BW = O + C + H + N + Ca + P + S + K + Na + Cl + Mg
Whole body/molecular	BW = lipids + water + protein + Mo + Ms + glycogen
Whole body/molecular	BW = fat + fat-free body mass
Whole body/cellular	BW = cell mass + extracellular fluids + extracellular solids
Whole body/tissue system	BW = adipose tissue + skeletal muscle + bone + viscera + blood + R
Whole body/whole body	BW = head + neck + trunk + lower extremities + upper extremities

<sup>a</sup>All units are in kilograms. Abbreviations: TB, total body; Mo, bone mineral; BW, body weight; Ms, soft tissue mineral; R, residues.

0.77; K/intracellular water = 150 mmol/liter; and H/body weight = 0.10 (65, 72). These known relationships, or rules, allow development of body composition models for estimating unknown components, such as protein = measured N/0.16 or N × 6.25 (14). Associations between components based on chemical bonds (i.e. covalent and ionic) are among the most stable used in body composition research and often form the basis of reference methods. For example, in humans, the proportion of bone as mineral is relatively stable, even in patients with osteoporosis (38). The main constituent of bone mineral is calcium hydroxyapatite, and calcium is therefore a stable proportion of bone mineral and bone (39). As less than 1% of total body calcium is found in soft tissues, measurement of calcium provides an accurate means of quantifying bone mineral in vivo.

Nonchemical elemental associations, such as the concentration of potassium in intracellular water, are relatively stable in healthy individuals but may show larger deviations with some diseases. Accordingly, total body potassium can be used to estimate intracellular water volume and body cell mass in healthy adults and in patients with stable fluid and electrolyte balance (57). On the other hand, intracellular potassium concentrations may undergo large alterations in

end-stage diseases and in conditions in which severe electrolyte disturbances are present. This underscores the important interactions between the areas of methodology and biological effects in body composition research. For example, one could not rely on measured total body potassium for estimating body cell mass in an end-stage AIDS patient in whom severe diarrhea and malnutrition produced serious acid-base and electrolyte disturbances.

### *Measurement Methods*

Elements are typically quantified for the whole body or in specific regions. The exchangeable ( $e$ ) mass of some elements can also be measured, such as for sodium ( $\text{Na}_e$ ) and potassium ( $\text{K}_e$ ) (22). The exchangeable compartment of an element is typically defined as the element's volume of distribution, usually measured with a radioisotope, over a specified period of equilibration. Lastly, it is possible to measure the distribution volume of some exogenously administered elements, as for example bromide ( $\text{Br}^-$ ), which has a dilution volume similar to the more-difficult-to-measure endogenous chloride distribution volume (67).

The 11 main elements and exogenously administered elements such as bromide can be measured *in vivo* by one or more methods. All *in vivo* human body composition methods, including those for elements, are ultimately based on measurable and relevant radioactive, electromagnetic, and physiological properties (76).

Once measured, a property must be mathematically transformed into the component mass of interest. The transformation process requires use of a mathematical function, and two main types can be arbitrarily defined (10a, 76). The first function type is based on an empirically derived relationship between the component and measured property. A reference method is used to estimate the component in a well-defined subject group in whom the property is also measured. A statistically derived component-prediction equation is developed and then cross-validated in a new subject group. We refer to these component-prediction equations as descriptive or type I mathematical functions (10a, 76). There are a large number of property-based prediction formulas for atomic level components (20).

The second type of mathematical function is based on stable relationships between properties and components, many of which can be understood in terms of their underlying biological basis. We refer to this category as mechanistic or type II mathematical functions (76), and there are many examples for atomic and higher level components. Some stable associations used in atomic and higher level component estimation formulas are summarized in Table 3. The development and validation of type II models is one of the most active areas of body composition research.

**Table 3** Examples of body composition methods<sup>a</sup>

Category	Equation	Reference method	Reference
Type I property-based methods	Fat = $0.65 \times BW - 0.21 \times Ht + 14.1$ FFM = $0.85 \times Ht^2/Z + 3.04$ SM = $18.9 \times Cre + 4.1$	Anthropometry Bioimpedance analysis 24-h urinary creatinine excretion	51 75 7
Type II property-based methods	Fat = $4.95 \times BV - 4.50 \times BW$ FFM = $5.50 \times BW - 4.95 \times BV$	Hydrodensitometry Hydrodensitometry	7
Type I component-based methods	Protein = $0.335 \times TBW - 2.53$	Tracer dilution	5
Type II component-based methods	Protein = $6.25 \times TBN$ FFM = $1.37 \times TBW$ BCM = $213 \times TBK$ Fat = $1.30 \times TBC - 4.45$ × $TBN - 0.06 \times TBCa$	Prompt- $\gamma$ IVNA Tracer dilution Whole-body <sup>40</sup> K counting Prompt- $\gamma$ IVNA and inelastic neutron scattering	14 59 56 45

<sup>a</sup>Abbreviation: BW, body weight; Ht, height; FFM, fat-free body mass; Z, electrical impedance; SM, skeletal muscle; Cre, 24-h urinary creatinine excretion; BV, body volume; TBW, total body water; TB, total body; BCM, body cell mass; IVNA, in vivo neutron activation.

A classic type II property-based atomic level method, and a good example, is estimation of total body potassium from the measured  $\gamma$ -ray decay of naturally occurring  $^{40}\text{K}$  (22). Potassium is predominantly nonradioactive  $^{39}\text{K}$ , although a small proportion (0.0118%) consists of radioactive  $^{40}\text{K}$ . This mixture of potassium isotopes also occurs in human tissues, and the 1.46-MeV  $\gamma$ -decay of  $^{40}\text{K}$  can be measured in whole-body counters of variable design. Once the subject's  $^{40}\text{K}$  amount is known, total body potassium (TBK, in millimoles) can be estimated as  $\text{TBK} = ^{40}\text{K}/0.0118\%$  (22).

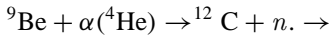
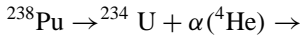
Some atomic and higher level components can be estimated from other known components by using type I or type II mathematical functions. These are referred to as component-based methods, and there are a number of them for estimating the 11 main atomic level elements (76). Representative examples of types I and II property- and component-based methods are presented in Table 3.

**IN VIVO NEUTRON ACTIVATION ANALYSIS** The most important development in measuring atomic level components occurred with accidental radiation exposure following nuclear reactor accidents in 1945 and 1946 (40). Ten subjects were exposed to neutron and  $\gamma$ -ray bursts, following which induced  $^{24}\text{Na}$  in their bodies was used as a measure of radiation exposure. Anderson and colleagues subsequently used controlled neutron irradiation for estimating total body Na and Cl in vivo (2). A number of methods have collectively descended from these seminal studies; they are referred to as in vivo neutron activation (IVNA) analysis (5, 12, 13, 18, 20).

As with accidental radionuclide exposure, controlled neutron irradiation induces release of  $\gamma$ -rays from tissue nuclei, and these  $\gamma$ -rays have element-specific detectable energies. Neutron activation analysis methods can quantify all of the main elements found in vivo, including total body H, C, N, O, Na, Ca, P, and Cl (52). Total body K can be measured with  $^{40}\text{K}$  whole-body counting, a procedure included as part of some IVNA protocols.

Neutrons ( $n$ ) are uncharged nuclear particles with a mass of 1. A number of methods produce controlled neutron beams of varying energy that are useful in IVNA systems. An important feature of neutrons is their intensity, usually estimated as the amount of energy per unit of time crossing a unit of area, expressed as kilo electron volts per square meter per second. Neutrons can be characterized as fast or high energy (>10 keV to 20 MeV) and low energy or thermal (0.2 eV to 10 keV). Fast neutrons are optimum for tissue penetration and favor some forms of neutron-nuclear interactions. Most neutron-nuclear interactions of importance to IVNA methods, however, occur with thermal neutrons. Neutron activation systems, therefore, include a fast-neutron source and rely on neutron thermalization with tissue interactions.

While there are many possible IVNA neutron sources, several examples will provide an overview of general concepts. An important neutron source is  $^{238}\text{PuBe}$ , which spontaneously undergoes the so-called  $\alpha$ - $n$  reaction:



Alpha particles, consisting of two neutrons and two protons, are equivalent to the helium nucleus. The resulting fast neutrons are  $\sim 3.5$  MeV (13).

Another approach is available for generating fast neutrons with a miniature accelerator (45). Deuterons, the nucleus (neutron + proton) of the stable isotope deuterium ( $^2\text{H}_2\text{O}$ ), are accelerated inside a small sealed tube until they reach a tritium ( $^3\text{H}_2\text{O}$ ) target. The deuterium-tritium fusion reaction results in helium production and release of 14 MeV neutrons. The neutron generator tube must be replaced when component isotopes are exhausted.

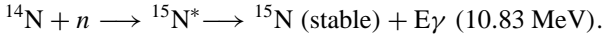
Produced fast neutrons interact with tissue nuclei and are absorbed or they escape from the system through free surfaces (66). Some neutrons lose energy by scattering as they collide with tissue elemental nuclei. The main scattering reaction is elastic, primarily with abundant hydrogen nuclei, and part of the neutron's kinetic energy is transferred to the incident nucleus and the remainder remains with the recoiling neutron. This reaction is denoted  $(n, n')$  as incident particle and emitted particle. Elastic scattering reactions transfer a large proportion of neutron energy to incident hydrogen protons as hydrogen is the most abundant nucleus, the two particles are similar in mass, and hydrogen has a large collision cross section. Higher energy neutrons, those at or above about 6 MeV, also can undergo inelastic scattering, in which some of the neutron's kinetic energy is converted to internal nuclear energy and in the process excites the incident nucleus with rapid  $\gamma$ -ray release  $(n, n'\gamma)$ .

Fast neutrons flowing across tissues, thus, are either absorbed or moderated by a series of elastic and inelastic collisions until thermal equilibrium is reached. The produced thermal neutrons rapidly diffuse through tissues and are captured within a few hundred microseconds by elemental nuclei. This radiative capture increases the element's mass by one nucleon and results in  $\gamma$ -ray release at energies specific to the incident element (12). This important reaction is denoted  $(n, \gamma)$  in the physics literature.

Two types of neutron-nuclear interactions, thus, produce  $\gamma$ -rays that are useful in IVNA: inelastic scattering with fast neutrons, and radiative capture with thermal neutrons. Three representative systems in use at Brookhaven National Laboratory (BNL), Long Island, provide good examples of the main IVNA methods in current use (17, 52).

*Prompt- $\gamma$ , neutron activation* The BNL prompt- $\gamma$  neutron activation system is currently used to measure total body H and N (17, 52). Neutrons with average energy,  $\sim 3.5$  MeV, are released by a collimated  $^{238}\text{PuBe}$  source positioned beneath the recumbent subject. A deuterium premoderator ensures uniformity of neutron flux. Radiative thermal neutron capture for  $^{14}\text{N}$  produces activated  $^{15}\text{N}^*$

$$\sim 10^{-15} \text{ s}$$



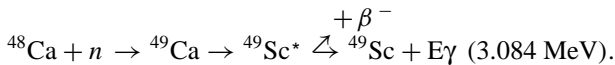
Activated  $^{15}\text{N}^*$  decays rapidly, producing stable  $^{15}\text{N}$  and releasing in the process a characteristic 10.83 MeV  $\gamma$ -ray.  $\gamma$ -Rays produced in the reaction are counted simultaneously with irradiation, and because their release is rapid ( $\sim 10^{-15}$  s), the method is referred to as prompt- $\gamma$  in vivo neutron activation analysis. Sodium iodide detectors quantify produced  $\gamma$ -rays. Two spectral peaks are measured, H at 2.223 MeV and N at 10.83 MeV.

Prior to IVNA evaluation, the subject's total body water is measured by tritium or deuterium dilution. Anthropometric measurements are also made, and equations are then used to estimate the subject's total body H (17, 52, 66). Hydrogen is then used as an internal standard to estimate total body N. Using hydrogen as an internal standard eliminates some of the technical concerns related to body habitués.

Scans are typically carried out from shoulder to knee and require about 1 h for completion. The coefficient of variation (CV) for repeated phantom measurements is 2.8% for total body N with a radiation exposure of 80 mrem.

*Delayed- $\gamma$  neutron activation* Some thermal neutron capture reactions produce radionuclides with relatively short half-lives. The decay of these radionuclides with consequent  $\gamma$ -ray emission can be measured within a short time interval ( $\sim 5$ – $20$  min) following irradiation. This approach is referred to as delayed- $\gamma$  neutron activation analysis because counting occurs following irradiation.

The BNL delayed- $\gamma$  neutron activation system is currently used to measure total body Ca, P, Na, and Cl (17, 52). Fast neutrons of  $\sim 3.5$  MeV are generated with 14 encapsulated  $^{238}\text{PuBe}$  sources positioned above and below the recumbent subject, who rests for 5 min inside the irradiation chamber. The subject is irradiated with fast neutrons and the reaction for calcium, for example, is

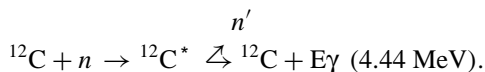


The notation for this reaction is given as  $[^{48}\text{Ca}(n, g)^{49}\text{Sc}]$  for [target nucleus

(incident particle, emitted particle) residual nucleus]. The irradiated subject is then moved to a counting area within 5 min, where the 3.084-MeV  $\gamma$ -rays from  $^{49}\text{Ca}$  decay are measured in the shielded BNL  $\gamma$ -ray spectrometer over an  $\sim 8$ -min period. Measured counts are converted to absolute total body Ca values by calibration with an anthropomorphic phantom with enclosed artificial skeleton. The phantom is designed for analysis of components, such as total body Ca, that are not uniformly distributed throughout the body.

The CV for total body Ca measurement by delayed- $\gamma$  neutron activation analysis is 1.5%, with a radiation exposure of 575 mrem. The delayed- $\gamma$  BNL system also allows measurements of total body Cl, Na, and P with CVs of 1.7%, 1.6%, and 2.5%, respectively.

*Inelastic neutron scattering* The inelastic neutron scattering system at BNL is used for measuring total body C and O. Incoming fast neutrons that interact with matter by inelastic collisions result in prompt nuclear deexcitation with  $\gamma$ -ray release ( $n, n'\gamma$ ). The reaction for carbon is



Increasing the energy of produced neutrons augments the probability of inelastic scattering reactions, such as this one for carbon, that have fast-neutron thresholds.

The BNL inelastic neutron scattering system is based on a miniature D,T sealed-tube, pulsating (4–10 kHz) neutron generator positioned beneath the recumbent subject. The 4.44-MeV  $\gamma$ -rays produced by inelastic scattering of C are detected by two bismuth germanate crystals positioned on each side of the subject. Detected counts measured over 30 min as the subject moves over the neutron cloud in both supine and prone positions are converted to total body C based on reference phantom calibrations. The BNL inelastic neutron scattering system CV is 3.0% for total body C, with a radiation exposure of 50 mrem.

*Representative protocol* The three BNL IVNA systems and whole-body counter are all located near each other. Subjects arrive in the early morning and are given an informed consent to sign. They are then evaluated for total body K in the whole-body counter and for tritium dilution volume. The estimate of tritium dilution volume is used in developing the total body water component for multicompartments models and also contributes with anthropometric measurements to derivation of total body H. The subject's predicted total body H is used as an internal standard for total body N estimation by prompt- $\gamma$  neutron activation analysis. The three IVNA studies are then completed, and

subjects are discharged in the early afternoon. The collective studies allow measurement of total body H, C, N, Na, K, Ca, Cl, and P.

The BNL systems are representative of IVNA installations throughout the world (5, 6, 12, 13, 66). Each system has special characteristics, although all are based on  $\gamma$ -ray release with neutron tissue-matter interactions.

*Role in body composition research* Neutron activation systems are costly and require a skilled group of investigators to maintain and operate. As a result, there are only a few centers in the world that have resources similar to those at BNL. The importance of these facilities is that elemental analysis allows reliable and reproducible reconstruction of molecular level components such as total body fat, protein, and mineral (38). This important characteristic of IVNA methods positions them as uniquely qualified to serve as reference methods, particularly in conditions in which unstable component associations render many currently available methods inaccurate.

## MOLECULAR LEVEL

Molecular level body composition components are integral to research in many nutrition areas, including energy, protein, and lipid metabolism, bone mineral homeostasis, and water balance.

### *Components and Their Relationships*

The many different chemical compounds found in the human body can be classified into five main groups: lipids, water, proteins, carbohydrates (i.e. glycogen), and minerals (Figure 2) (77). Subfractions of components can also be defined, as for example the triacylglycerol or fat portion of lipid, the extra and intracellular portions of total body water, and bone and soft-tissue minerals.

Lipids are defined as chemical compounds that are soluble in lipid solvents such as diethyl ether and chloroform (29). The most abundant lipid species in humans are the triacylglycerols, which generically are often referred to as fats. Some authors inaccurately use the term fat in reference to total lipids, adding some confusion to the published literature. The non-fat lipids include phospholipids, sphingolipids, and steroids. In humans triacylglycerols or nonessential lipids are energy storage compounds, while the remaining lipid species are essential in various biochemical and physiological processes.

Water is mixed with electrolytes *in vivo* and bound ionically to varying degrees with protein, glycogen, and other polar chemical compounds. Water is distributed into the intracellular and extracellular compartments, and the extracellular water compartment includes five subcompartments: interstitial, plasma, connective tissue, bone, and gastrointestinal tract (22, 76).

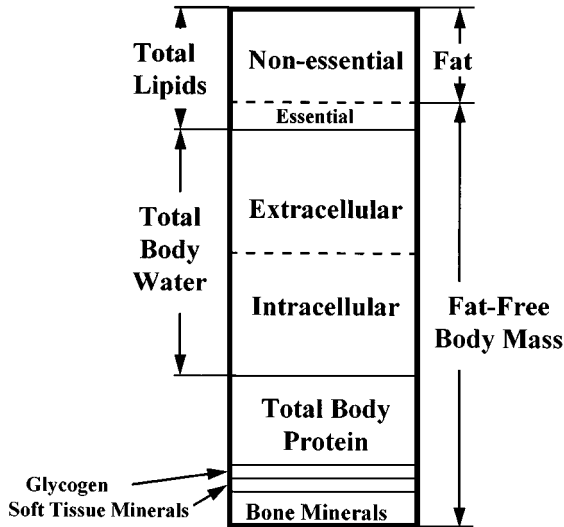


Figure 2 Molecular level components.

There are many different families of proteins, but noninvasive body composition methods are available only for estimation of total protein (14) and muscle and non-muscle proteins (13).

There is less than 1 kg of glycogen in healthy adults; the remaining carbohydrates are considered negligible (16, 72). The two main intracellular glycogen pools are in liver (~1% wet weight) and skeletal muscle (~2% wet weight) (72). Until recently, most of the available information on glycogen in vivo was obtained with biopsies of selected muscle groups. The growing availability of nuclear magnetic resonance spectroscopy systems for human use is providing new noninvasively obtained information on the amount of and dynamic changes in intracellular glycogen (44).

Minerals comprise about 5% of body weight in healthy adults and are distributed in two main compartments: bone minerals and non-bone or soft-tissue minerals. The main constituent of bone minerals is calcium hydroxyapatite  $[Ca_3(PO_4)_2]_3Ca(OH)_2$  (38), with small contributions made by Na, K, Mg, and Cl. Soft-tissue minerals include well-known ions such as  $Na^+$ ,  $K^+$ ,  $Cl^-$ ,  $HPO_4^{2-}$ , and  $HCO_3^-$  (38).

Although there are five main molecular level components, it is common to combine components in order to develop body composition methods. For example, the molecular level can be described as any of the following combinations: a two-compartment model in which body weight (BW) = fat + fat-free body

mass, and  $BW = \text{lipid} + \text{lipid-free body mass}$ ; a three-compartment model in which  $BW = \text{fat} + \text{water} + \text{residual}$  (i.e. the sum of glycogen, minerals, and protein) (76), and  $BW = \text{fat} + \text{bone mineral} + \text{lean soft tissue}$ ; and a four-compartment model in which  $BW = \text{fat} + \text{water} + \text{minerals} + \text{residual}$  (i.e. the sum of glycogen and protein). There still remains some uncertainty in these various models on inclusion of the nontriacylglycerol essential lipid component.

Many stable relationships recognized for the molecular level are integral to the body composition methodology area (Table 1). One of the most important features of molecular level components from the methodology perspective is their physical density. This is because whole-body density is relatively easy to measure accurately in most children and healthy adults (26), and many molecular level models are based on density or closely related body volume (39, 49). Three components—water, glycogen, and triacylglycerols (i.e. fat)—are homogeneous or approach homogeneous chemical moieties from the body composition viewpoint. Accordingly, their densities at body temperature were easily established by early investigators using conventional gravimetric methods. Protein, bone mineral, and soft-tissue mineral are heterogeneous with respect to composite amino acids, minerals, and electrolytes, and their densities were more difficult to estimate. Representative bone samples, for example, can be exposed to  $>500^{\circ}\text{C}$  for a prolonged period, and the density of the remaining ash can be measured with gravimetric methods (38).

The density of combined components such as fat-free body mass can be calculated by assuming relatively stable proportions among the various constituent chemical components (7). The calculated and assumed constant densities of combined molecular level components are the basis of two-, three-, and four-component molecular level models, which are formulated on body density or volume measured with underwater weighing (7) or newer air displacement plethysmograph systems (55).

Other important stable relationships at the molecular level include the hydration (59) and potassium content (22) of fat-free body mass (Table 2).

### *Measurement Methods*

There are many methods for estimating molecular level components. As some of these methods are reviewed in detail elsewhere (62), we concentrate on recent methodological developments.

Some measurable body properties—such as impedance to an electrical current, attenuation of X-rays, and ultrasonic waves, body weight, and body volume—can be used in developing molecular level methods (22). We now examine several of these methods, with the aim of reviewing their underlying physical basis and application in the broader area of body composition methodology.

**BIOIMPEDANCE ANALYSIS** Bioimpedance analysis (BIA), the subject of an extensive multi-author publication organized by the Nutrition Coordinating Center at the National Institutes of Health, has important potential as a field body composition method (23). Most body composition methods are costly and difficult to transport and require specialized teams for their maintenance and optimum performance. In contrast, BIA systems are usually inexpensive, easy to carry from one site to another, and simple to operate. BIA, therefore, is a useful supplement to anthropometry.

In the BIA method, an alternating current at one or more frequencies is introduced via electrodes across a tissue bed, and impedance (voltage drop) to electrical flow is detected. Impedance is the opposition of tissue to current flow and is the inverse of conductance. Electrolyte-rich fluids such as body water pose the least impedance to electrical flow, while lipids and bone minerals provide the most (3). Accordingly, impedance and its two main components, resistance and reactance, are primarily determined by the volume of fluid present in the electrical pathway. Many BIA prediction formulas at specific electrical frequencies are available for estimation of total body water and its two main subcompartments, extracellular and intracellular water (23). Fluids and water form relatively stable relationships with other components, and BIA methods are often designed to quantify fat-free body mass and, indirectly, fat (i.e. body weight minus fat-free body mass). All currently used BIA approaches are type I, which are reference-method dependent.

In the standard whole-body BIA method, electrodes are placed on the hand and foot, although increasing attention is focusing on segmental measurements, since impedance appears to be determined mainly by the arms and legs. Stringent measurement conditions are recommended for BIA, and prediction formulas must always be validated (23). There is growing use of BIA in field studies of body composition, and a rapidly expanding area is the use of impedance methods for clinically evaluating subjects with altered hydration, such as dialysis patients (23).

An important limitation of BIA methods is that many underlying assumptions are required, and some of these either have not yet been adequately explored or are known to be inaccurate. For example, traditional BIA methods employ a geometric model that assumes the component of interest is homogeneous in composition and uniform in cross-sectional area (50, 51). The typical electrical pathways used with BIA in humans fail to conform to such idealized conditions.

Similar concerns related to BIA validity are now undergoing critical analysis by investigators actively engaged in body composition research. Bioimpedance methods, therefore, should be used only under appropriate and carefully controlled conditions.

**DUAL ENERGY X-RAY ABSORPTIOMETRY** Francis Moore, one of the pioneers in body composition research, tried with limited success 30 years ago to estimate skeletal weight in vivo (57). The introduction of IVNA for total body calcium measurement in 1964 (2) led to the first analysis of bone in living subjects. However, IVNA exposes subjects to radiation, and studies in healthy children and young women are not usually recommended. A new strategy for estimating bone mineral was introduced in 1963 by Cameron & Sorenson (11). A radionuclide source was placed on one side of a subject's wrist, a location with minimal soft tissue, and a photon detector was placed on the opposite side of the wrist. Atomic interactions between radionuclide-emitted photons and elements within bone mineral attenuated the photon beam, and reduced flux was measured in the photon detector. The technique, which became known as single photon absorptiometry, was an important development in the assessment of wrist bone mineral content.

The bone mineral content of the hip and spine are also important in the study of osteoporosis. Photons passing through soft tissues overlying hip and vertebral bones are attenuated not only by bone minerals but by soft tissues as well. The problem of non-bone photon attenuation was solved by treating the photon pathway as a two-component mixture consisting of bone minerals and soft tissue. Two photon energies, typically provided by radionuclide sources, were used to estimate the bone mineral and soft-tissue content of each pixel. Known originally as dual-photon absorptiometry, the recent use of X-ray photon sources led to methods collectively referred to as dual energy X-ray absorptiometry (DXA) (54). Moore's hope of measuring the skeleton has been fulfilled on a wide scale. Most large hospitals in the United States have available DXA systems for whole-body and regional bone mineral evaluation.

In order to solve for pixel bone mineral, DXA systems must also establish attenuation characteristics of overlying soft tissues. These characteristics, expanded upon in the following sections, also allow estimation of fat and fat-free soft tissues. Most DXA systems with appropriate software are therefore now capable of estimating whole-body and regional bone mineral, fat, and fat-free soft tissues (Figure 3). As extremity fat-free soft tissue is mainly muscle, except for a small amount of skin and connective tissue, DXA also is capable of providing appendicular skeletal muscle mass estimates (37).

The DXA physical concept is not complicated, although actual implementation and software development is complex. The system X-ray source produces a polychromatic photon spectrum. Two main energy peaks are then created using one of two strategies: electrically pulsing the X-ray tube, or allowing the X-rays to pass across a rare earth cerium or samarium k-edge filter (73). Exponential attenuation of photons occurs as they pass across the subject's tissues secondary to two main types of interaction, Compton scattering and

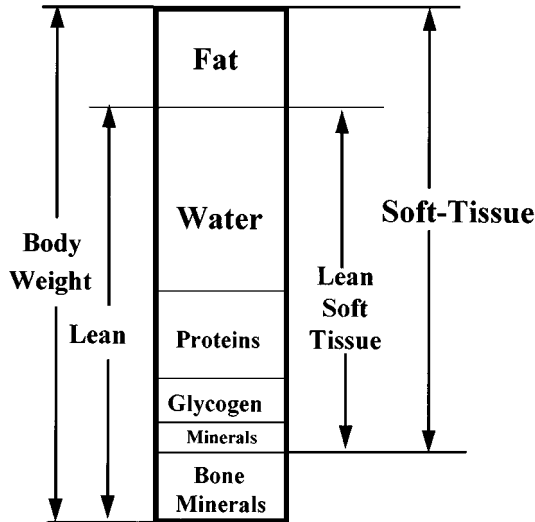


Figure 3 DXA molecular level model. The lean component as shown in the figure is equivalent to fat-free body mass. (From Reference 60 with permission.)

photoelectric effect (42, 43, 73, 78). Diminished photon intensity for each of the energies is recorded by appropriately positioned detectors. The attenuation characteristics are used to estimate the fraction of each component in the evaluated pixel: soft tissue plus bone mineral in pixels with bone; and fat plus lean soft tissue in pixels with soft tissue alone.

X-ray attenuation in human tissues at typical DXA energies is related mainly to the type and proportion of elements present and to photon energy (28). Elements with low atomic numbers (e.g. H and C) minimally attenuate photons, while elements with higher atomic numbers (e.g. Ca and P) strongly attenuate photons. As photon energy is increased, there is less photon attenuation.

The degree to which an element attenuates photons can be expressed as an experimentally measured constant referred to as the mass attenuation coefficient. Each element has a characteristic mass attenuation coefficient ( $\mu/\rho$ ) at any specified photon energy. It can be shown mathematically that the ratio of photon attenuation at DXA's two main energies for any element is equivalent to the ratio of the element's energy-specific mass attenuation coefficients. Mass attenuation coefficients can also be calculated for chemical level components according to their elemental composition.

A convenient expression that relates attenuation at the two DXA energies is the *R* value, which is the ratio of attenuation at the low- to high-energy peak

(28). For example, the  $R$  value for a hypothetical pure hydrogen tissue would be equal to the ratio of hydrogen's energy-specific mass attenuation coefficients. At typical energies, such as 40 and 70 keV,  $\mu/\rho$  for hydrogen are 0.3458 and 0.3175 with an  $R$  value of 1.0891. For complex mixtures, such as are present with real tissues, the measured  $R$  value reflects the mass fraction of each element present (60).

In concept, DXA systems measure the  $R$  value of each pixel (27, 60). When considering only those pixels with soft tissue, fat has a relatively large amount of lower- $R$  carbon ( $R = 1.2199$ ), whereas lean soft tissue has a relatively large amount of higher- $R$  oxygen ( $R = 1.4167$ ), nitrogen ( $R = 1.3043$ ), and residual electrolytes and minerals (Figure 4). For the Reference Man (72), the theoretical  $R$  values for fat and lean soft tissue at 40 and 70 keV are 1.21 and 1.37, respectively. Fat and lean, thus, have different elemental proportions and  $R$  values. A phantom, consisting of animal soft tissues, can be made with varying amounts of fat and lean. When scanned, there will be a highly significant correlation between measured  $R$  and the proportion of phantom soft tissue as fat (60).

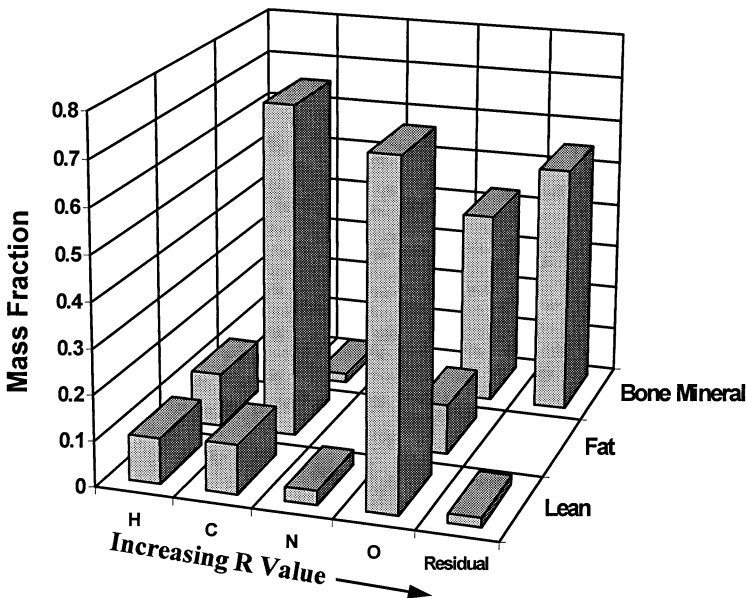


Figure 4 Mass fraction of main elements in lean soft tissues, fat, and bone mineral based on Reference Man (72). Residual mass represents the sum of Na, Mg, P, S, Cl, K, Ca, and trace elements. The respective calculated  $R$  values at 40 and 70 keV for fat, lean, and bone mineral are 1.21, 1.37, and 2.86, respectively (60).

Thus, the phantom, or some other similar calibration standard, can be used to develop either an  $R$  value prediction equation or by extrapolation specific pure fat and lean  $R$  values. Alternatively, prediction equations based on measured  $R$  values can be developed in vivo for body fat or closely related adipose tissue. How to appropriately calibrate and cross-validate DXA systems is an important question now receiving the attention of a number of investigators. Calibrated DXA systems can thus provide estimates of fat and lean for soft tissue pixels.

Pixels that contain bone require a different analytical strategy. There exist in each of these pixels three components: fat, lean soft tissue, and bone mineral. With two energies, DXA in theory can only resolve a two-component mixture, as was shown for soft tissue. The  $R$  value for pure bone mineral is easily ascertained from human bone or other similar phantoms. However, soft-tissue composition is variable in fat, and therefore the  $R$  value for soft tissue overlying bone cannot be assumed constant. In the first analytical step following the DXA scan, pixels with and without bone are easily identified by using several mathematical procedures, including the recognition that bone minerals have a high  $R$  value and that measured pixels with high  $R$  values most likely contain bone. The  $R$  value for soft tissue overlying bone is estimated using mathematical modeling procedures and is based on the measured soft-tissue  $R$  on either side of the bone (60). With the soft-tissue and bone mineral  $R$  values now known, the amount of fat, lean soft tissue, and bone mineral in the pixel can be ascertained. This DXA analytical strategy thus allows estimation of three components based on measured attenuation of two main energy peaks.

Although there are many variable characteristics of DXA systems, all share in common the assumed elemental proportions of fat, lean, and bone mineral components, each with known and constant attenuation characteristics (Figure 4). Thus, DXA is a property-based type II method.

Many studies have now examined DXA accuracy and reproducibility in both animals and humans. With respect to accuracy, DXA fat and bone mineral estimates in species ranging widely in body size are highly correlated with corresponding criterion estimates, such as chemical analysis of cadavers and IVNA. In some cases there exists bias between DXA and criterion estimates, although this problem is often considered a correctable calibration problem. Body composition estimates by DXA usually are highly reproducible, with repeated measurements over one day in the same subject demonstrating CVs of about 1% for total body bone mineral, 2% for fat-free soft tissue, and 0.8% for fat (56).

**MULTICOMPARTMENT MODELS** Until recently, whole-body chemical analysis of human cadavers was required for establishing the accuracy of in vivo methods and for exploration of relationships between components. Cadaver analysis remains important, but investigators are increasingly able to simultaneously

measure several chemical compartments in an individual subject by using multicompartment models.

There are many published multicompartment models, and more are possible. All multicompartment models share in common their development from simultaneous equations, which may include two or more unknown components. As a general rule, for each unknown component estimated there must be one independent equation that includes the unknown component, the known component, and/or the measurable property. Measurable molecular level components include total body water by isotope dilution (22), total body protein by neutron activation of total body nitrogen (13), glycogen (regional) by nuclear magnetic resonance spectroscopy (44), and bone and soft-tissue minerals by activation of total body calcium (5, 18, 65), whole-body  $^{40}\text{K}$  counting (22), and DXA (54). Measurable properties used in developing molecular level multicomponent models include body weight and body volume.

A representative model for estimating total body fat from measured carbon and other elements begins with the following basic formula:

$$\begin{aligned} \text{Total body C} = & 0.77 \times \text{fat} + 0.53 \times \text{protein} + 0.444 \times \text{glycogen} \\ & + \text{C in bone mineral.} \end{aligned}$$

This model links atomic level carbon to molecular level components. The coefficients are assumed proportions of molecular level components as carbon. The next two models assume that protein is 16% nitrogen and that the ratio of glycogen to protein is constant, respectively:

$$\text{Protein} = 6.25 \times \text{total body nitrogen},$$

and

$$\text{glycogen} = 0.044 \times \text{protein}.$$

This fourth model assumes that the ratio of bone mineral carbon to bone mineral calcium is constant:

$$\text{Bone mineral in carbon} = 0.05 \times \text{bone mineral calcium}.$$

These four formulas can then be solved for fat mass as (45)

$$\text{fat} = 1.30 \times \text{TBC} - 4.45 \times \text{TBN} - 0.065 \times \text{TBCa}.$$

There are two important families of multicompartment models. The first of these, *in vivo* neutron activation analysis multicompartment models, evolved from the relatively simple four-compartment model:  $\text{BW} = \text{water} + \text{protein} + \text{mineral} + \text{fat}$  (32). Water in this model is usually estimated from tritium or deuterium dilution volumes. Protein and mineral are estimated from models based

**Table 4** Models for estimating total body fat mass based on measured body weight and volume<sup>a</sup>

Model	Measurable properties	Known components(s)	Reference
2-Compartment			
Fat = $4.95 \times BV - 4.50 \times BW$	BV, BW	none	7
3-Compartment			
Fat = $2.057 \times BV - 0.786 \times TBW - 1.286 \times BW$	BV, BW	TBW	70
4-Compartment			
Fat = $6.386 \times BV + 3.961 \times \text{mineral} - 6.09 \times BW$	BV, BW	mineral	48
Fat = $2.75 \times BV - 0.714 \times TBW + 1.148 \times \text{mineral} - 2.05 \times BW$	BV, BW	TBW, mineral	4
Fat = $2.75 \times BV - 0.714 \times TBW + 1.129 \times Mo - 2.037 \times BW$	BV, BW	TBW, Mo	68
Fat = $2.513 \times BV - 0.739 \times TBW + 0.947 \times Mo - 1.79 \times BW$	BV, BW	TBW, Mo	39

<sup>a</sup>Abbreviations: BV, body volume (liters); BW, body weight (in kilograms); TBW, total body water (in kilograms) Mo, bone mineral.

on total body N and Ca, respectively. Fat is usually an unknown component and is considered the difference between body weight and the three estimated components. Over the years this simple model was refined by investigators to include separate estimates for bone and soft-tissue minerals and glycogen (32, 38). One of the more recent advances is the addition of total body fat estimates from total body carbon using a similar model to the one presented above (38).

A good example of neutron activation analysis model implementation is the BNL six molecular level-compartment model. Over the course of about 4 h, subjects complete whole-body counting, tritium dilution, and prompt- $\gamma$ , delayed- $\gamma$ , and inelastic scattering neutron activation analysis studies. Eleven elements are measured or calculated, as noted earlier, and from these elements six molecular level compartments are derived (fat, protein, glycogen, water, soft-tissue minerals, and bone minerals).

The second family of molecular level multicompartiment models, those based on body volume estimation, derives from the observation that physical densities of molecular level components are known and relatively constant at body temperature. Examples of these models that are used to estimate total body fat are presented in Table 4.

Behnke and his colleagues in 1942 first introduced the modern underwater weighing method as a means of estimating body density (7). Behnke and others who followed developed two-compartment models for estimating fat and fat-free body mass from measured body volume and body weight. The model was expanded to three compartments by Siri in 1961, who added total body water estimates to measured body volume and weight to derive fat and residual mass (i.e. protein, glycogen, and minerals) (70). The introduction of dual photon methods for estimating bone minerals in the past decade allowed development

of four-compartment models (i.e. fat, water, minerals, and combined protein plus glycogen), some of which are summarized in Table 4.

A typical four-compartment study requires several hours for completion, usually beginning with isotope dilution for total body water and measurement of body weight. Underwater weighing and DXA studies then follow for body volume and bone mineral estimation, respectively. Four measured variables—total body water, body weight, body volume, and bone mineral mass—are then used to calculate total body fat. The mass of glycogen is often considered negligible in four-component calculations, as the amount present, particularly after an overnight fast, is relatively small. The underwater weighing technique required for developing multicompartment body volume models are found in many centers throughout the world.

Multicompartment models are used in body composition research when investigators are interested in examining the effects of physiological or other processes on several compartments. Another application is when accurate component estimates are desired, particularly in unstable or non-steady state conditions. Fat estimates by the conventional two-compartment model would not be accurate following an intervention that produces disproportionate fluid accumulation. This is because the two-compartment model assumes stable fat-free body mass hydration. In contrast, some models used in multicompartment methods tend to be more stable and are usually insensitive to altered fluid balance and other similar effects. For example, the method of estimating total body fat from carbon, nitrogen, and calcium is unaltered in accuracy regardless of the subject's hydration. Multicompartment models are also used at other body composition levels.

## CELLULAR LEVEL

There are over  $10^{18}$  cells in the human body that are bathed in extracellular fluid and supported by a framework of extracellular solids. The cell level's importance is centered primarily on the protoplasmic or intracellular compartment, which is the site of most metabolic processes.

### *Components and Their Relationships*

The traditional cellular level model consists of three components: cell mass, extracellular fluid, and extracellular solids (Figure 1). The extracellular solids are not of much clinical interest, as they consist mainly of bone minerals and collagen, reticular, and elastic fibers (77). Extracellular fluid is slightly larger than extracellular water, also a molecular level component, as it includes dissolved electrolytes and proteins. The cell mass component is of interest primarily for the metabolically active protoplasm that includes cytoplasmic organelles and mitochondria found within the intracellular space. Adipocytes, and to a small

extent other cells, store triacylglycerols within the intracellular compartment. Moore and his colleagues in the 1960s introduced the body cell mass concept as a means of quantifying the metabolically active fat-free portion of the intracellular space (57). Today the most widely used cellular level model is  $BW = \text{fat} + \text{extracellular fluid} + \text{extracellular solids} + \text{body cell mass}$ .

There are many relatively stable cellular-level relationships that are used in body composition research, and some of the more important of these are as follows:  $K/\text{intracellular water} = 159 \text{ mmol of K/kg of H}_2\text{O} = 6.22 \text{ g of K/kg of H}_2\text{O}$ ;  $K/\text{body cell mass} = 4.69 \text{ g/kg}$ ;  $\text{Ca}/\text{extracellular solids} = 0.177 \text{ kg/kg}$ ; and  $\text{extracellular water}/\text{extracellular fluid} = 0.92$ .

### *Measurement Methods*

Body cell mass is the most important measurable component at the cellular level. Conceptually, body cell mass consists of two portions: an intracellular fluid component, and an intracellular solid component. There are no methods available for estimating intracellular solids. The usual approach in estimating body cell mass is to assume a stable relationship between measurable intracellular fluid and unmeasurable intracellular solids. Alternatively, investigators report only their measurements of intracellular fluid as an index of the body cell mass component.

Two strategies are employed for intracellular fluid measurement. The first is to assume that potassium is distributed mainly into the intracellular compartment and maintains a relatively constant concentration of 150 mmol/liter. There are three main methods of quantifying body potassium: whole-body  $^{40}\text{K}$  counting; dilution of  $^{42}\text{K}$  or  $^{43}\text{K}$ ; and as the exchangeable component estimated from total body water, exchangeable sodium, and serum water/electrolytes (69). The second approach is to calculate intracellular water by using multicomponent models based on total body water and extracellular water estimates. A number of dilution methods are available for estimating total body and extracellular water components (22). Calculation of body cell mass from intracellular fluid or water assumes a constant proportion of body cell mass as intracellular solids. The classic body cell mass formula of Moore et al (57), which is based on total body or exchangeable K, assumes that all of measured K is intracellular, that the  $K/\text{intracellular water}$  is 150 mmol/liter, and that intracellular water/body cell mass is about 0.80. Accordingly,  $\text{body cell mass} = \text{total body K (mmol)} \times 0.0083$ .

## TISSUE-SYSTEM LEVEL

### *Components and Their Relationships*

The main tissue-system level components are adipose tissue, skeletal muscle, bone, visceral organs, and brain. Adipose tissue is further divided into

subcutaneous, visceral, yellow marrow, and interstitial subcomponents (72, 77).

Some reasonably stable relations at the tissue-system level include: skeletal muscle/adipose tissue free body mass = 0.54 (for men) or 0.49 (for women); K/skeletal muscle = 3 g/kg; fat/adipose tissue = 0.8; and bone mineral/bone = 0.54 (72).

### *Measurement Methods*

**THREE-DIMENSIONAL IMAGING** Until recently, estimation of tissue-system level components was accomplished with relatively inaccurate methods such as anthropometry. Today, both computerized axial tomography (CT) and MRI can quantify all major tissue-system level components (Figure 1). Two-dimensional standard radiography was first used to capture adipose tissue and skeletal muscle shadows by Stuart and colleagues in the early 1940s (74). By the beginning of the 1950s, radiogrammetry, as it was called, allowed investigators to estimate subcutaneous adipose tissue layer thickness and muscle widths (25). Hounsfield introduced three-dimensional CT for brain imaging in 1971 and first reported his seminal observations in 1973 (41). The method proliferated rapidly, and by the late 1970s, CT systems were installed in most major medical centers. Heymsfield and colleagues between 1979 and 1981 reported the use of CT to measure skeletal muscle mass, visceral organ volumes, and visceral adipose tissue (31, 33–35). Borkan and his group reported their classic visceral adipose tissue studies with CT in 1982 (10), and in 1986, Kvist et al published for the first time assessment of whole-body adipose tissue volumes with multislice CT (47). The method reported by Kvist et al in Sweden involved preparation of 22 or more cross-sectional CT images at well-defined anatomic locations followed by calculating total volumes of various body composition components by integration of appropriate slice areas and distance between slices.

MRI and its precursor, nuclear magnetic resonance spectroscopy, originated with the fundamental studies of Bloch et al (9) and Purcell et al (61), reported in 1946. By the early 1970s, Damadian was preparing images of phantoms using proton nuclear magnetic resonance signals (15). Early clinical applications of MRI using small bore magnets were first reported in 1978, and within a few years, several researchers described a variety of MRI procedures using whole-body large bore magnets (53). The utility of MRI to discriminate between anatomical structures in both the abdomen and the musculoskeletal regions was first reported in the early 1980s. By the mid-1980s, MRI systems became available in hospitals throughout North America.

Foster et al (23a) were the first to use MRI in body composition research when, in 1984, they demonstrated in cadavers that MRI could distinguish between adipose tissue and skeletal muscle. Hayes and colleagues in 1988 first

characterized with MRI subcutaneous adipose tissue distribution in human subjects (30). In 1991, Fowler et al obtained 28 MRIs over the whole body (24), and in 1992, Ross et al reported a 41-image model for measuring adipose and lean tissue distribution (64). Both CT and MRI are now widely used for regional and whole-body analysis of tissue-system level components.

CT and MRI are composed of picture elements, pixels, which are usually squares  $1\text{ mm} \times 1\text{ mm}$  and which have a third dimension related to slice thickness. Volume elements are referred to as voxels. Voxels have a gray scale that reflects tissue composition and provides image contrast. Component estimates by both CT and MRI are expressed as volumes unless they are subsequently converted to mass units by assuming constant tissue densities (e.g. 0.92 kg/liter for adipose tissue and 1.04 kg/liter for skeletal muscle).

CT systems consist of a rotating X-ray tube and detector, which move in a perpendicular plane to the subject. The CT X rays are attenuated as they penetrate tissues and Fourier analysis or filtered back-projection are used in reconstructing the image. The CT number, assigned to each pixel, is a measure of photon attenuation relative to air and water (71). Air [ $-1000$  Hounsfield units (HU)], adipose tissue ( $-90$  to  $-30$  HU), non-adipose lean tissues ( $-29$  to  $+151$  HU), and skeleton ( $+152$  to  $+2500$  HU) pixels all have characteristic CT number ranges that allow their separation into specific tissue areas within a cross-sectional image. Tissue areas can be used in monitoring the same subject over time or in comparing subjects to each other. Combining information from multiple slices allows reconstruction of a whole organ or whole-body tissue volume.

The fundamental MRI concept is based on interaction between nuclei of abundant hydrogen atoms and magnetic fields produced and controlled by the system's instrumentation. Protons, the hydrogen nucleus, have a magnetic moment that causes them to function as small magnets. Under usual conditions in the earth's weak magnetic field, these magnetic moments are randomly oriented, and they tend to cancel each other. When a subject is placed inside the scanner's high-field strength magnet proton, magnetic moments tend to align themselves longitudinally to the external magnet's field. A pulsed radio-frequency (RF) field is then applied to body tissues, causing some of the aligned hydrogen protons to absorb energy. Switching off the RF field allows protons to gradually assume their original positions and to release in the process absorbed energy. This signal generated by energy release is used to create MRIs.

The time ( $T$ ) it takes for the protons to return to their original positions is a function of two parameters, longitudinal relaxation time ( $T_1$ ) and transverse relaxation time ( $T_2$ ). The longitudinal relaxation time is a constant that is dependent on the interaction between relaxing proton spin and the surrounding medium. The  $T_1$  for protons in fat is much shorter ( $\sim 1/4$ ) when compared with  $T_1$  values for protons in water, and therefore it is possible to generate

images with good adipose and non-adipose tissue contrast. Optimum image contrast requires selection of an RF pulse sequence that properly exploits the  $T_1$  differences between the two tissues. This is accomplished by varying what are known as the RF pulse time-to-repeat ( $TR$ ) and time-to-echo ( $TE$ ) parameters. One such sequence, spin-echo, varies the  $TR$  parameter to take advantage of  $T_1$  differences and, thus, provides the tissue contrast required to generate high-quality images. The  $T_1$ -weighted spin-echo RF pulse sequence is commonly used in body composition research.

The  $T_2$  parameter is a time constant related to the interaction between relaxing proton spins. The  $T_2$ -weighted images are used to characterize the acute effects of exercise on skeletal muscle (36).

To obtain MRI data, the subject is positioned in the magnet's bore in either a prone or a supine position. Typically, a 320-mm region of the body is imaged in a single acquisition. The time required to obtain multiple (i.e. seven) images is the same as that required to obtain a single image. Therefore, in most MRI studies, multiple images of a given region are obtained in a single acquisition. The procedures typically are used to acquire MRI data over the whole body, and an example of images obtained in the abdomen and appendicular regions are presented in Figure 5. Note that the MRI pulse-sequence used to image the

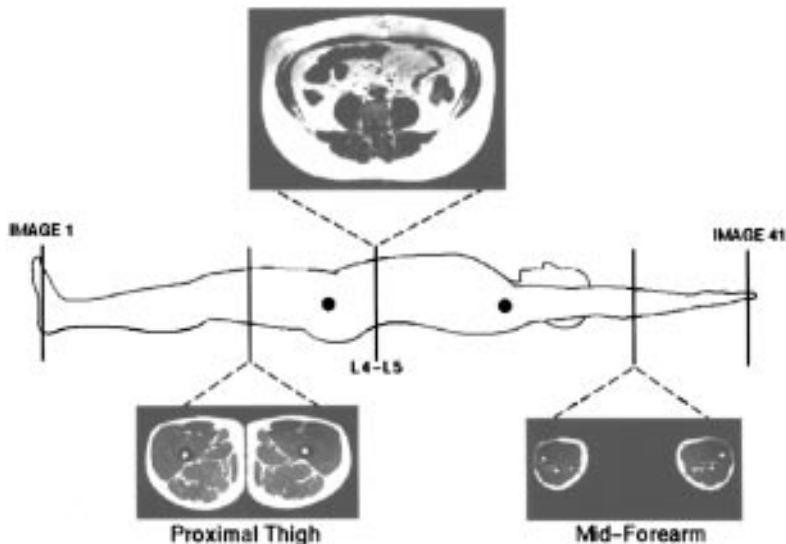


*Figure 5* Three magnetic resonance images in a healthy adult, one from the abdomen and two from the appendicular region. The images were acquired using a  $T_1$ -weighted, spin-echo pulse sequence. With this protocol, adipose tissue appears white and non-adipose tissue is dark on all images.

abdominal region requires 26 s. During this time the subject is asked to hold his or her breath, a procedure that substantially reduces respiratory motion artifacts.

In the published literature, MRI data appear either as areas (square centimeters), obtained from a single image, or as volumes (cubic centimeters), derived by using tissue area measurements from multiple images. The first step in tissue area measurement is to count the number of pixels that make up the tissue of interest (36). The tissue area is subsequently determined by multiplying the number of pixels by their known area. The volume of a tissue for the whole body or a given region is derived in two steps. First, the volume for each image is obtained by multiplying the area of the tissue by image thickness. Whole-body or regional volume is then calculated by using a mathematical formula that sums truncated cone volumes defined by pairs of consecutive images.

The CV for repeated measures of subcutaneous adipose tissue ranges from 1% to 10% (36). The CV for visceral adipose tissue estimates is higher, 6% to 11%, as a result of measurement errors associated with respiratory motion. For skeletal muscle, the CV for repeated measurements in the appendicular region ranges from 0.3% to 2.3%.

*Validation* There are extensive validation studies for CT and MRI, which include phantoms and human and animal cadavers. In this section, we provide several representative examples of CT and MRI validation experiments.

Imaging methods can be evaluated in phantoms and excised organs and tissues. Water-filled balloons, excised human kidneys, livers, and spleens, and organs from two human cadavers were examined by multislice CT (31, 33–35). The mean absolute difference between actual weight and CT-derived weight was 2.6%, 4.6%, and 5.6% for balloons, excised organs, and in situ organs, respectively. In another cadaver experiment, Rossner and colleagues (65) compared adipose tissue estimates by CT with corresponding planimetry measurements of corresponding band-sawed slices from two male cadavers. There were strong correlations between the two types of area estimates ( $r = 0.77$ – $0.94$ ). Human cadavers were also used by Abate et al (1) to examine the validity of MRI abdominal subcutaneous and visceral adipose tissue estimates. The overall agreement between dissection weight and MRI-estimated adipose tissue weights was 6%.

There are many animal CT and MRI validation studies. For example, Ross et al examined whole-carcass chemically extracted lipid in rodents and found a good correlation with MRI-adipose tissue mass ( $r = 0.97$ ,  $P < 0.01$ ) (63). There are also CT and MRI validation studies in larger animals, such as pigs, and here, too, the overall agreement between chemical analysis and imaging method is good.

Taken collectively, these studies support the validity of regional and total-body CT and MRI tissue-system level estimates.

*Interpretation* The recent study of Bhasin and colleagues demonstrates some important aspects of CT and MRI data interpretation (8). The investigators induced skeletal muscle growth with supraphysiologic doses of testosterone in normal men. Hormone-treated men showed a significant increase in an MRI-measured quadriceps cross-sectional area ( $P < 0.001$ ), whereas muscle area changes were nonsignificant in placebo-treated men. While the inference of these observations is that the observed increase in quadriceps muscle area reflects anabolic effects of androgens in stimulating deposition of new myofibrillar proteins, there are other possibilities as well. For example, the increase in quadriceps muscle area might represent expansion of the muscle glycogen pool and water volume. A full interpretation of MRI-detected increase in skeletal muscle area would require additional studies of body composition and, potentially, chemical analysis of skeletal muscle biopsies.

## METHOD SELECTION

### *Reference Method*

An important quest in body composition research is to find the best reference method, or the gold standard. Although weighing of organs or chemical analysis of human cadavers provides the most accurate measure of most components, only a few complete cadaver analyses have been carried out, and there are many technical problems with this approach.

The next consideration in selecting a reference method is that it must be appropriate for the body composition level and component under study. For example, fat is a molecular level component and adipose tissue is a tissue-system level component. Adipose tissue measured by MRI would therefore not be expected to serve as a reference comparison against which fat estimates by a method such as underwater weighing are compared.

Type I body composition methods are developed against established reference methods. For example, anthropometry, BIA, infrared interactance, and ultrasound include error from the reference method. Type I methods, therefore, are not acceptable reference standards.

Type II body composition methods, such as some neutron activation analysis methods, DXA, underwater weighing, and MRI are often cited as in vivo reference standards. Judging the suitability of a reference method requires an analysis of errors arising from two main sources, model and technical. Some models are extremely stable whereas others are not (77). For example, models based on chemical relationships (e.g.  $N/protein = 0.16$ ) are very stable under almost all circumstances. Models developed with nonchemical relationships (e.g.  $total\ body\ water/fat-free\ body\ mass = 0.732$ ) are less stable and are

often influenced by disease, pregnancy, and other conditions that deviate from “normal.” There are many sources of technical error, and a few examples are instrument calibration, instrument stability, subject participation, and observer variation. Weighing the contribution of these many factors to total method error is a very difficult but important task.

The final consideration is that reference body composition methods must be available to investigators if they are to be useful. There are thus many factors to consider when choosing a reference body composition method.

### *Study Method*

The method selected for a specific project depends mainly on the study hypothesis or clinical application. Is the method suitable for individual or group evaluations? Will the method give accurate component results in the group under investigation? That is, are prediction equations for type I methods appropriate for the study population? Are models used in type II methods appropriate for use in the study population? Are regional or whole-body measurements needed? Is the method sufficiently reliable to detect hypothesized changes over time? Important additional considerations in method selection include instrument or reagent cost, safety, and portability (e.g. laboratory or field study). Information beyond that presented in this review can be found in body composition textbooks (22, 62).

## CONCLUSION

Remarkable progress is evident in the field of body composition research. While not long ago only a few components could be measured in vivo, today most major components at the first four levels of body composition can be accurately measured in an individual subject. The timing of these advances is opportune, as major nutritional questions require body composition estimates for their full examination.

## ACKNOWLEDGMENTS

We acknowledge the suggestions of Drs. Ruimei Ma and Angelo Pietrobelli in manuscript preparation. This work was supported by National Institutes of Health Grant RO1-AG 13021.

Visit the *Annual Reviews* home page at  
<http://www.annurev.org>.

## Literature Cited

1. Abate N, Burns D, Peshock RM, Garg A, Grundy SM. 1994. Estimation of adipose tissue mass by magnetic resonance imaging: validation against dissection in human cadavers. *J. Lipid Res.* 35:1490-96
2. Anderson J, Osborn SB, Tomlinson RWS, Newton D, Rundo J, et al. 1964. Neutron-activation analysis in man in vivo: a new technique in medical investigation. *Lancet* 2:1201-5
3. Baumgartner RN, Chumlea WC, Roche AF. 1990. Impedance for body composition. *Exerc. Sport Sci. Rev.* 18:193-224
4. Baumgartner RN, Heymsfield SB, Lichtman S, Wang J, Pierson RN. 1991. Body composition in elderly people: effect of criterion estimates on predictive equations. *Am. J. Clin. Nutr.* 53:1345-53
5. Beddoe AH, Hill G. 1985. Clinical measurement of body composition using in vivo neutron activation analysis. *J. Parent. Enter. Nutr.* 9:504-20
6. Beddoe AH, Stereat SJ, Hill GL, Knight GS. 1985. New approaches to clinical assessment of lean body tissues. In *Body Composition Assessments in Youth and Adults*, ed. AF Roche, pp. 62-72. Columbus, OH: Ross Labs.
7. Behnke AR, Feen BG, Welham WC. 1942. The specific gravity of healthy men. *J. Am. Med. Assoc.* 118:495-98
8. Bhasin S, Stores TW, Berman N, Callegari C, Clevenger B, et al. 1996. The effects of supraphysiologic doses of testosterone on muscle size and strength in normal men. *N. Engl. J. Med.* 335:1-7
9. Bloch F, Hansen WW, Packard ME. 1946. Nuclear introduction. *Phys. Rev.* 70:460-74
10. Borkan GA, Gerzof SG, Robbins AH, Hulth DE, Silbert CK, Silbert JE. 1982. Assessment of abdominal fat content by computerized tomography. *Am. J. Clin. Nutr.* 36:172-77
- 10a. Brown D, Rothery P. 1993. *Models in Biology: Mathematics, Statistics and Computing*, p. 13. Sussex, UK: Wiley
11. Cameron JR, Sorenson J. 1963. Measurement of bone mineral in vivo. *Science* 42:230-32
12. Chettle DR, Fremlin JH. 1984. Techniques of in vivo neutron activation analysis. *Phys. Med. Biol.* 29:1011-43
13. Cohn SH. 1981. In vivo neutron activation analysis: state of the art and future prospects. *Med. Phys.* 8:145-53
14. Cunningham J. 1994.  $N \times 6.25$ : recognizing a bivariate expression for protein balance in hospitalized patients. *Nutrition* 10:124-27
15. Damadian R. 1971. Tumor detection by nuclear magnetic resonance. *Science* 171:1151-53
16. Diem K. 1962. *Documenta Geigy Scientific Tables*, Geigy Pharmaceuticals. New York: Ardsley. 778 pp.
17. Dilmanian FA, Weber DA, Yasumura S, Kamen Y, Lidofsky L, et al. 1990. Performance of the neutron activation systems at Brookhaven National Laboratory. In *Advances in Vivo Body Composition Studies*, ed. S Yasumura, KG McNeill, AD Woodhead, FA Dilmanian. New York: Plenum
18. Dutton J. 1991. In vivo analysis of body elements and body composition. *Univ. Wales Sci. Tech. Rev.* 8:19-30
19. Ellis KJ. 1990. Reference man and woman more fully characterized. Variations on the basis of body size, age, and race. *Biol. Trace Elem. Res.* 26-27:385-400
20. Ellis KJ. 1996. Whole-body counting and neutron activation analysis. See Ref. 62, pp. 45-62
21. Fielding RA. 1996. Effects of exercise training in the elderly: impact of progressive resistance training on skeletal muscle and whole-body protein metabolism. *Proc. Nutr. Soc.* 54:665-75
22. Forbes GB. 1987. *Human Body Composition*. New York: Springer-Verlag
23. Foster KR, Lukaski HC. 1996. Whole-body impedance—what does it measure? *Am. J. Clin. Nutr.* 64:S388-96
- 23a. Foster MA, Hutchison JMS, Mallard JR, Fuller M. 1984. Nuclear magnetic resonance pulse sequence and discrimination of high- and low-fat tissues. *Magn. Reson. Imaging* 2:187-92
24. Fowler PA, Fuller MF, Glasby CA, Foster MA, Cameron GG, et al. 1991. Total and subcutaneous AT distribution in women: the measurement of distribution and accurate prediction of quantity by using magnetic resonance imaging. *Am. J. Clin. Nutr.* 54:18-25
25. Garn SM. 1957. Roentgenogrammetric determination of body composition. *Hum. Biol.* 29:337
26. Going SB. 1996. Densitometry. See Ref. 62, pp. 3-24
27. Gotfredsen A, Borg J, Christiansen C, Mazess RB. 1984. Total body bone mineral in vivo by dual photon absorptiometry. I. Measurement procedures. *Clin. Physiol.* 4:343-55

28. Gotfredsen A, Jensen J, Borg J, Christiansen C. 1986. Measurement of lean body mass and total body fat using dual photon absorptiometry. *Metab. Clin. Exp.* 35:88-93
29. Gurr MI, Harwood JL. 1991. *Lipid Biochemistry*. London: Chapman & Hall. 4th ed.
30. Hayes PA, Sowood PJ, Belyavin A, Cohen JB, Smith FW. 1988. Subcutaneous fat thickness measured by magnetic resonance imaging, ultrasound, and calipers. *Med. Sci. Exerc.* 20:303-9
31. Heymsfield SB, Fulenwider T, Nordlinger B, Balow R, Sones P, Kutner M. 1979. Accurate measurement of liver, kidney, and spleen volume and mass by computerized axial tomography. *Ann. Intern. Med.* 90:185-87
32. Heymsfield SB, Lichtman S, Baumgartner RN, Wang J, Kamen Y, et al. 1990. Body composition of humans: comparison of two improved four-compartment models that differ in expense, technical complexity, and radiation exposure. *Am. J. Clin. Nutr.* 52:52-58
33. Heymsfield SB, Noel R. 1981. Radiographic analysis of body composition by computerized axial tomography. In *Nutrition and Cancer*, ed. N Ellison, G Newell, 17:161-72. New York: Raven
34. Heymsfield SB, Noel R, Lynn M, Kutner M. 1979. Accuracy of soft tissue density predicted by CT. *J. Comput. Assist. Tomogr.* 3:859-60
35. Heymsfield SB, Olafson RP, Kutner MH, Nixon DW. 1979. A radiographic method of quantifying protein-calorie undernutrition. *Am. J. Clin. Nutr.* 32:693-702
36. Heymsfield SB, Ross R, Wang ZM, Frager D. 1997. Imaging techniques of body composition: advantages of measurement and new uses. In *Emerging Technologies for Nutrition Research*, pp. 1-25. Washington, DC: Natl. Acad. Press. In press
37. Heymsfield SB, Smith R, Aulet M, Bensen B, Lichtman S, et al. 1990. Appendicular skeletal muscle mass: measurement by dual-photon absorptiometry. *Am. J. Clin. Nutr.* 52:214-18
38. Heymsfield SB, Waki M, Kehayias J, Lichtman S, Dilmannian FA, et al. 1991. Chemical and elemental analysis of humans in vivo using improved body composition models. *Am. J. Physiol.* 261: E190-98
39. Heymsfield SB, Wang ZM, Withers R. 1996. Multicomponent molecular-level models of body composition analysis. See Ref. 62, pp. 129-48
40. Hoffman JG, Hempelmann LH. 1957. Estimation of whole-body radiation doses in accidental fission bursts. *Am. J. Roentgenol.* 77:144-60
41. Hounsfield GN. 1973. Computerized transverse axial scanning (tomography). *Br. J. Radiol.* 46:1016
42. Hubbell JH. 1969. Photon cross sections, attenuation coefficients, and energy absorption coefficients from 10 keV to 100 GeV. In *US Natl. Bur. Stand., The Supt. Doc.*, pp. 1-85. Washington, DC: US Gov. Print. Off.
43. Hubbell JH. 1982. Photon mass attenuation and energy-absorption coefficients from 1 KeV to 20 MeV. *J. Appl. Radiat. Isot.* 33:1269-90
44. Jue T, Rothman DL, Shulman GI, Tavitian BA, DeFronzo RA, Shulman RG. 1989. Direct observation of glycogen synthesis in human muscle with <sup>13</sup>C NMR. *Proc. Natl. Acad. Sci. USA* 86:4489-91
45. Kehayias JJ, Heymsfield SB, LoMonte AF, Wang J, Pierson RN Jr. 1991. In vivo determination of body fat by measuring total body carbon. *Am. J. Clin. Nutr.* 53:1339-44
46. Krentz AJ, Koster FT, Crist DM, Finn K, Johnson LZ, et al. 1993. Anthropometric, metabolic, and immunological effects of recombinant human growth hormone in AIDS and AIDS-related complex. *J. Acquired Immune Defic. Syndr.* 6:245-51
47. Kvist H, Sjöström L, Tylén U. 1986. Adipose tissue volume determinations in women by computed tomography: technical consideration. *Int. J. Obes.* 10:53-67
48. Lohman TG. 1986. Applicability of body composition techniques and constants for children and youths. *Exerc. Sport Sci. Rev.* 14:325-57
49. Lohman TG. 1992. *Advances in Body Composition Assessment*. Champaign, IL: Hum. Kinet.
50. Lukaski H. 1989. Applications of bioelectric impedance analysis: a critical review. In *In Vivo Body Composition Studies: Recent Advances*, ed. S Yasumura, JE Harrison, KE McNeill, AD Woodhead, FA Dilmannian, pp. 365-74. New York: Plenum
51. Lukaski HC, Johnson PE, Bolonchuk WW, Lykken GI. 1985. Assessment of fat-free mass using bioelectrical impedance measurement of the human body. *Am. J. Clin. Nutr.* 41:810-17
52. Ma R, Dilmannian FA, Rarback H, Stamatelatos IE, Meron M, et al. 1993. Recent upgrade of the IVNA facility at BNL. In *Human Body Composition, In Vivo Methods, Models, and Assessment*, ed. KJ

- Ellis, JD Eastman, pp. 345–50. New York: Plenum
53. Mansfield P, Pykett IL, Morris PG. 1978. Human whole body line-scan imaging by NMR. *Br. J. Radiol.* 51:921–22
  54. Mazess RB, Barden HS, Bisek JP, Hanson J. 1990. Dual-energy X-ray absorptiometry for total-body and regional bone-mineral and soft-tissue composition. *Am. J. Clin. Nutr.* 51:1106–12
  55. McCrory MA, Gomez TD, Bernauer EM, Mole PA. 1995. Evaluation of a new air displacement plethysmograph for measuring human body composition. *Med. Sci. Sports Exerc.* 27:1686–91
  56. Modlesky CM, Lewis RD, Yetman KA, Rose B, Roskopf LB, et al. 1996. Comparison of body composition and bone mineral measurements from two DXA instruments in young men. *Am. J. Clin. Nutr.* 64:669–76
  57. Moore FD, Oleson, KH, McMurray, JD, Parker HV, Ball MR, et al. 1963. *The Body Cell Mass And Its Supporting Environment*. Philadelphia: Saunders
  58. Ogle GD, Rosenberg AR, Kainer G. 1992. Renal effects of growth hormone. II. Electrolyte homeostasis and body composition. *Pediatr. Nephrol.* 6:483–89
  59. Pace N, Rathbun EN. 1945. Studies on body composition. III. The body water and chemically combined nitrogen content in relation to fat content. *J. Biol. Chem.* 158:685–91
  60. Pietrobelli A, Formica C, Wang ZM, Heymsfield SB. 1996. Dual-energy X-ray absorptiometry body composition model: review of physical concepts. *Am. J. Physiol.* 271:E941–51
  61. Purcell EM, Torrey HC, Pound RV. 1946. Resonance absorption by nuclear magnetic moments in a solid. *Phys. Rev.* 69:37–38
  62. Roche AF, Heymsfield SB, Lohman TG, eds. 1996. *Human Body Composition*. Champaign, IL: Hum. Kinetics. 366 pp.
  63. Ross R, Léger L, Guardo R, dDe Guise J, Pike BG. 1991. Adipose tissue volume measured by magnetic resonance imaging and computerized tomography in rats. *J. Appl. Physiol.* 70:2164–72
  64. Ross R, Léger L, Morris D, de Guise J, Guardo R. 1992. Quantification of adipose tissue by MRI: relationship with anthropometric variables. *J. Appl. Physiol.* 72:787–95
  65. Rossner S, Bo WJ, Hiltbrandt E, Hinson W, Karstaedt N, et al. 1990. Adipose tissue determinations in cadavers: a comparison between cross-sectional planimetry and computed tomography. *Int. J. Obes.* 14:893–902
  66. Ryde SJS, Birks JL, Morgan WD, Evans CJ, Dutton J, et al. 1993. A five-compartment model of body composition of healthy subjects assessed using in vivo neutron activation analysis. *Eur. J. Clin. Nutr.* 47:863–74
  67. Schoeller DA. 1996. Hydrometry. See Ref. 62, pp. 25–44
  68. Selinger A. 1977. *The Body as a Three Component System*. PhD thesis. Univ. Ill., Urbana
  69. Shizgal HM, Spanier AH, Humes J, Wood CD. 1977. Indirect measurement of total exchangeable potassium. *Am. J. Physiol.* 233:F253–59
  70. Siri WE. 1961. Body composition from fluid spaces and density: analysis of methods. In *Techniques for Measuring Body Composition*, ed. J Brozek, A Henschel, pp. 223–44. Washington, DC: Natl. Acad. Sci. Natl. Res. Council.
  71. Sjöström L. 1991. A computer-tomography based multicomponent body composition technique and anthropometric predictions of lean body mass, total and subcutaneous adipose tissue. *Int. J. Obes.* 15:19–30
  72. Snyder WM, Cook MJ, Nasset ES, Karhausen LR, Howells GP, Tipton IH. 1975. *Report of the Task Group on Reference Man*. Oxford: Pergamon
  73. Sprawls P Jr. 1977. *The Physical Principles of Diagnostic Radiology*. Baltimore: Univ. Park
  74. Stuart HC, Hill P, Shaw C. 1940. The growth of bone, muscle and overlying tissue as revealed by studies of roentgenograms of the leg area. *Monogr. Soc. Res. Child Dev.* 5(No. 3, Ser. 26):1–190
  75. Wang ZM, Gallagher D, Nelson ME, Matthews DE, Heymsfield SB. 1996. Total body skeletal muscle mass: evaluation of 24-h urinary creatinine excretion by computerized axial tomography. *Am. J. Clin. Nutr.* 63:863–69
  76. Wang ZM, Heshka S, Pierson RN Jr, Heymsfield SB. 1995. Systematic organization of body composition methodology: overview with emphasis on component-based methods. *Am. J. Clin. Nutr.* 61:457–65
  77. Wang ZM, Pierson RN Jr, Heymsfield SB. 1992. The five level model: a new approach to organizing body composition research. *Am. J. Clin. Nutr.* 56:19–28
  78. White DR, People LHJ, Crosby TJ. 1980. Measured attenuation coefficients at low photon energies (9.88–59.32 keV) for 44 materials and tissues. *Radiat. Res.* 84:239–52